Journal of Geophysical Research – Earth Surface

Supporting Information for

Measured basal water pressure variability of the western Greenland Ice Sheet: Implications for hydraulic potential

Patrick J. Wright[1], Joel T. Harper[1], Neil F. Humphrey[2], and Toby W. Meierbachtol[1]

[1]Department of Geosciences, University of Montana, Missoula, MT, USA

[2]Department of Geology and Geophysics, University of Wyoming, Laramie, WY, USA

Contents of this file

Text S1 to S2
Figures S1 to S2

Introduction

Text S1 describes statistical techniques used to generate box plots and to calculate mean annual water pressure.

Text S2 and Figures S1 – S2 provide details of the methodology used in the analysis of hydraulic potential gradient sensitivity to diurnal pressure variations (as shown in Figure 10).

S1. Statistical techniques

Box plots were generated to summarize seasonal and diurnal water pressure datasets. For seasonal analysis, seven records encompass part or all of a single melt season, and five records include winter data, with four of these records spanning slightly more than a year (Table 1). For borehole records spanning part or all of a single melt season, box plots represent all data contained in the record, whereas the five records with winter data have been separated into box plot pairs for characteristic winter and melt season records, respectively. This approach allows for separate analysis of melt season and winter pressures, and allows calculation of an annual weighted mean pressure that incorporates data from all boreholes.

The borehole water pressure records show non-normal distributions, thus we use dataset medians as an indicator of central tendency for the temporal scale of interest. An annual mean value is calculated by weighting the mean melt season median among all boreholes to 3.5 months (0.29 yr), and the mean winter median among five boreholes to 8.5 months (0.71 yr). This weighting scheme allows the use of all records in the dataset, using a time span of characteristic melt season data for weighting that is generally consistent among all boreholes, from approximately June 15 to October 1. To avoid over-representation of periods with high sampling rates, all boxplots and reported median values are calculated from data re-sampled to the common long-term sampling rate (5 minute or 15 minute for melt season records, and 15 minute or 30 minute for winter records).

S2. Potential gradient sensitivity to diurnal pressure variations

In Discussion section 5.2.1 we calculate $\nabla\phi_h$ vectors using equation (4) with 250-m horizontal resolution bed and surface topography [*Lindbäck et al.*, 2014], and with an imposed high and low pressure to represent a diurnal cycle. The imposed range in pressure is derived from the largest measured range (5th to 95th percentile) represented in the twelve-borehole suite (range of 0.12 OB, measured in borehole 27km-12B). To more accurately represent the distribution of pressure measured throughout the transect, we then center the imposed range at the mean diurnal pressure median for all boreholes, resulting in an imposed diurnal range of 0.87 to 0.99 OB (shaded region in Figure 9).

Under this scenario, gradient vectors change both their magnitude and direction as a result of the diurnal pressure changes. Depending on the slope and aspect of underlying bed topography vectors can rotate up to 180° and both increase and decrease in magnitude. To demonstrate the limits of this process we initially explore the scenario for two borehole locations, testing both the imposed range of pressure and the maximum physically possible range of pressure (Figure S1).

We then apply the analysis to the entire study area at 250-m resolution using the imposed pressure range (represented by angle 2 in Figure S1). Resulting hydraulic potential vector pairs and the corresponding potential field contours for high and low pressure conditions are demonstrated for a section along the Issunguata Sermia trough wall (Figure S2). The ratio in magnitude and the rotation angle between the high and low pressure vectors is then calculated for the entire study area (Figure 10). This analysis does not represent actual water flow paths at the bed (which are complicated by local pressure and stress fields), but is intended to illustrate plausible changes in the magnitude and direction of $\nabla\phi_h$ due to diurnal pressure swings.

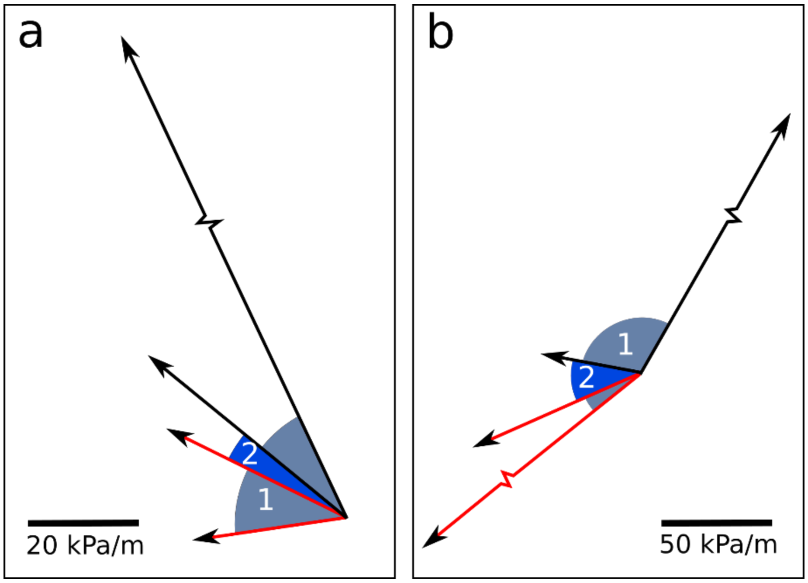

Figure S1. Changes in magnitude and rotation of hydraulic potential gradient vectors resulting from the physically possible range of basal water pressure (angle 1, 0.0 OB to 1.17 OB), and for the imposed range of water pressure used for diurnal analysis (angle 2, 0.87 OB to 0.99 OB). Red vectors and black vectors correspond to high-pressure and low-pressure conditions, respectively. Panel (a) uses the bed and surface topography from site 27km-12A, representing conditions commonly found over steep sub-glacial trough walls where vector magnitudes increase with decreasing pressure. Panel (b) uses the bed and surface topography from site M2-10B, representing conditions of reverse bed slope (bed aspect opposed to surface slope aspect), resulting in a decrease in vector magnitude with decreasing pressure.

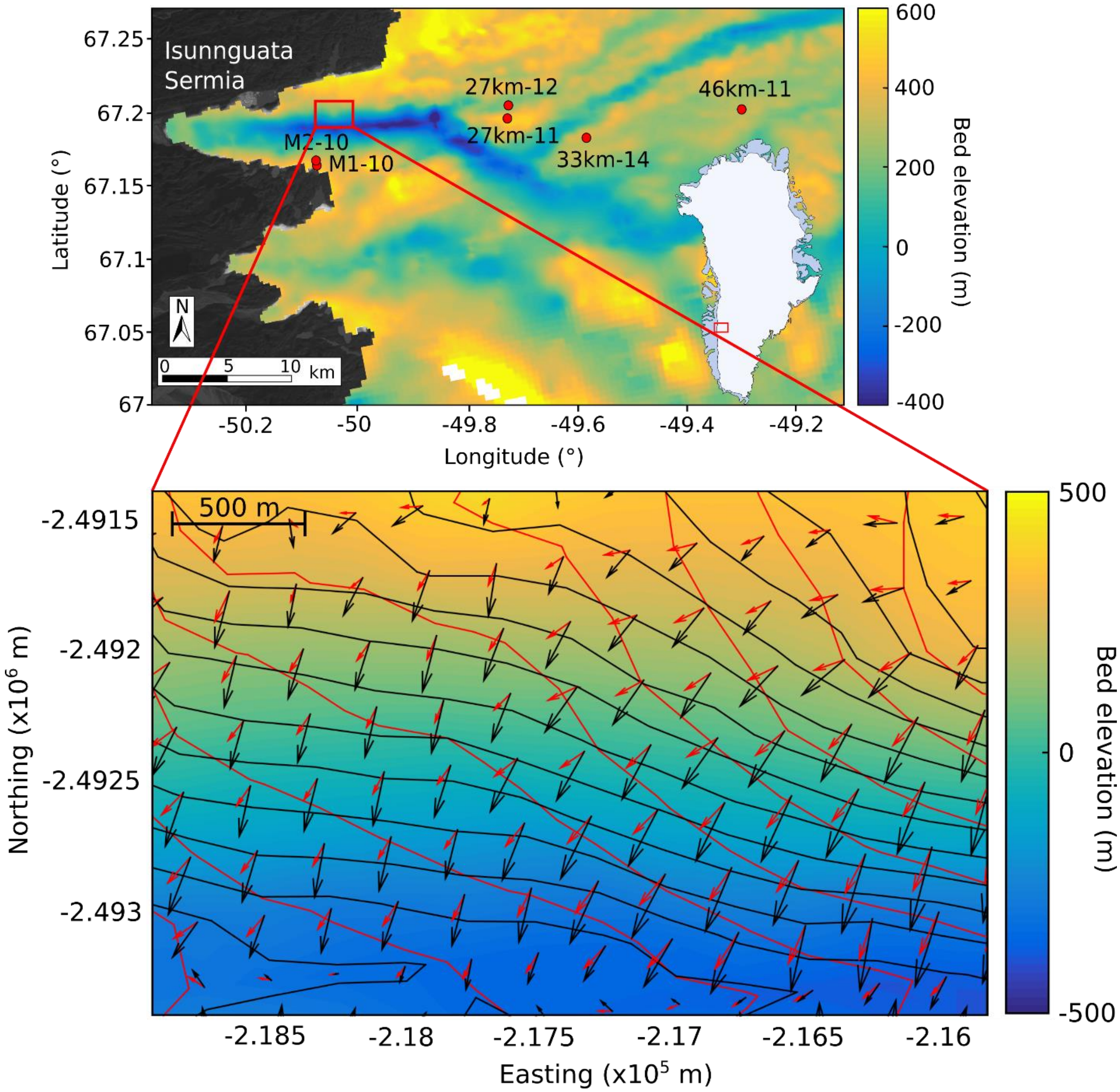

Figure S2. Modification of hydraulic potential gradient magnitude and direction for a section along the Issunguata Sermia trough wall, as forced by an imposed diurnal pressure range of 0.87–0.99 OB. Base colormap is derived from 250-m resolution bed topography [*Lindbäck et al.,* 2014]. Red vectors and contours represent the hydraulic potential gradient and surface, respectively, for high pressure conditions. Black vectors and contours represent low pressure conditions. The imposed pressure range is constrained by borehole observations, as shown in Figure 9.